Am J Physiol Heart Circ Physiol
280: H2920–H2928, 2001.

Nonlinear dynamics of heart rate variability in cocaine-exposed neonates during sleep

SMITA GARDE, MICHAEL G. REGALADO,
VICKI L. SCHECHTMAN, AND MICHAEL C. K. KHOO
Biomedical Engineering Department, University of Southern California, Los Angeles 90089; Department of Pediatrics, Cedars-Sinai Medical Center, Los Angeles 90048; and Brain Research Institute, University of California School of Medicine, Los Angeles, California 90095

Received 18 September 2000; accepted in final form 6 February 2001

Garde, Smita, Michael G. Regalado, Vicki L. Schechtman, and Michael C. K. Khoo. Nonlinear dynamics of heart rate variability in cocaine-exposed neonates during sleep. *Am J Physiol Heart Circ Physiol* 280: H2920–H2928, 2001.—The aim of this study was to determine the effects of prenatal cocaine exposure (PCE) on the dynamics of heart rate variability in full-term neonates during sleep. R-R interval (RRI) time series from 9 infants with PCE and 12 controls during periods of stable quiet sleep and active sleep were analyzed using autoregressive modeling and nonlinear dynamics. There were no differences between the two groups in spectral power distribution, approximate entropy, correlation dimension, and nonlinear predictability. However, application of surrogate data analysis to these measures revealed a significant degree of nonlinear RRI dynamics in all subjects. A parametric model, consisting of a nonlinear delayed-feedback system with stochastic noise as the perturbing input, was employed to estimate the relative contributions of linear and nonlinear deterministic dynamics in the data. Both infant groups showed similar proportional contributions in linear, nonlinear, and stochastic dynamics. However, approximate entropy, correlation dimension, and nonlinear prediction error were all decreased in active versus quiet sleep; in addition, the parametric model revealed a doubling of the linear component and a halving of the nonlinear contribution to overall heart rate variability. Spectral analysis indicated a shift in relative power toward lower frequencies. We conclude that *1*) RRI dynamics in infants with PCE and normal controls are similar; and *2*) in both groups, sympathetic dominance during active sleep produces primarily periodic low-frequency oscillations in RRI, whereas in quiet sleep vagal modulation leads to RRI fluctuations that are broadband and dynamically more complex.

autonomic function; cardiovascular control; infants; modeling

PRENATAL COCAINE EXPOSURE is believed to affect infant heart rate control and sleep-wake state organization. However, the number of studies that have investigated these effects are few, and the conclusions that have been drawn from the various data pools remain ambiguous (20). On one hand, some studies (21, 33) have found mean heart rate to be elevated and heart rate variability (HRV) to be reduced in infants with prenatal cocaine exposure. On the other hand, a recent study (23) found reduced median heart rates and increased HRV in cocaine-exposed neonates relative to controls. Spectral analysis of these data has shown that the higher HRV is due to increases in spectral power across all frequency bands in quiet sleep and increases in spectral power in the low-frequency (0.03–0.1 Hz) and mid-frequency (0.1–0.2 Hz) bands in active sleep (24). These results differ somewhat from the study of Oriol et al. (21), which found a significant reduction in high-frequency power.

The apparent discrepancy among these previous findings may be due in part to differences in the development of the subject groups that were studied as well as to the difficulty of controlling and determining the amount of prenatal cocaine exposure. Another possibility is that summary statistics and linear measures of heart rate dynamics may not be sufficiently sensitive to uncover differences in cardiovascular function between infants with prenatal cocaine exposure and controls without prior prenatal cocaine exposure. There may well be more subtle differences that become detectable only through methods that have the capability of characterizing the nonlinear aspects of the underlying dynamics. A number of studies (9, 11, 29) have suggested that the irregular behavior found in HRV may be a manifestation of deterministic chaos: complex dynamics that arise from nonlinear interactions among the many mechanisms that control or influence heart rate. However, other studies (7, 14), applying more stringent mathematical tests for chaos, found no evidence to support this hypothesis, although these researchers did find significant nonlinear correlations in the data. Recent findings by some groups (6, 13) suggest further that the irregular dynamics of HRV may be due in large part to stochastic influences.

In this study, we applied a variety of computational techniques to determine whether there are differences in the nonlinear dynamics of HRV of cocaine-exposed

Address for reprint requests and other correspondence: M. C. K. Khoo, Biomedical Engineering Dept., Univ. of Southern California, OHE-500, University Park, CA 90089-1451 (E-mail: khoo@bmsrs.usc.edu).

The costs of publication of this article were defrayed in part by the payment of page charges. The article must therefore be hereby marked "*advertisement*" in accordance with 18 U.S.C. Section 1734 solely to indicate this fact.

neonates and age-matched controls. We further hypothesized that the fluctuations in R-R interval (RRI) in both groups of neonates can be modeled as the output of a dynamic deterministic feedback system with stochastic noise as a possible perturbing input. Employing this structural framework, we sought to determine whether the dynamics of the feedback system could be adequately characterized by a linear model or whether it was necessary to include nonlinear contributions. Furthermore, this model allowed us to estimate the relative contributions of deterministic versus stochastic components to overall HRV in these two groups of infants during quiet and active sleep.

METHODS

Subjects. We studied 12 normal neonates and 9 infants with prenatal cocaine exposure. All infants were products of single births by vaginal delivery with birth weights of >2,500 g and Apgar scores at 5 min of >7. The birth weights of the two groups of infants [controls 3,415 ± 130 g (SE) vs. cocaine-exposed 3,528 ± 236 g] were not significantly different. All subjects were studied at 2 wk postpartum. The mothers of all the subjects were single African-American and Hispanic women. Cocaine exposure was determined by maternal self-report or neonatal toxicological urinalysis (EMIT procedure) in the perinatal period. Histories of current and past cocaine (reported in terms of frequency of use during each trimester of pregnancy), alcohol (reported as absolute ounces of alcohol per week during each trimester), and tobacco (reported as mean number of cigarettes per week during each trimester) use were taken from each woman at the time of the sleep recording according to the recommendations of Day et al. (8). The Obstetric Complications Scale (17) was completed for each participant. Mothers of the control infants tested negative for cocaine and were selected from the same population of single African-American and Hispanic women. Radioimmunoassay of the mothers' hair (3) was used to verify cocaine exposure and the lack thereof in the cocaine group and the control group, respectively. The study was approved by the institutional review board of the King-Drew Medical Center (Los Angeles, CA), and each participating mother gave written informed consent.

Measurements and data preprocessing. Four-hour daytime recordings of the electrocardiogram (ECG) were obtained from the infants during spontaneous sleep and wakefulness. These recordings were made between 0900 and 1500 hours. Each 1-min epoch (of a total of ~240 epochs) was classified as quiet sleep, active sleep, indeterminate sleep, or waking on the basis of behavioral criteria using a previously reported protocol (25). The intervals between successive R waves of the ECG (RRI) were determined with 1-ms accuracy by subtracting the time of each R wave from the time of the previous R wave. In each subject, we selected for analysis two artifact-free segments of RRI data of ~1,000 beats (8–10 min) duration each; one of these was from quiet sleep and the other was from active sleep. Care was taken to ensure that no state changes occurred within a given segment. Segments representing wakefulness were not included in our comparisons because we were unable to find a sufficiently large number of data segments (containing 1,000 contiguous beats) that were free of artifacts. During wakefulness, there was frequently crying or other behavioral activities that produced motion artifacts in the ECG recordings.

All the data sets were first linearly detrended. To test further for stationarity, each detrended data set was divided into segments of 1-min duration, and the means and standard deviations of the RRI in each segment were computed. Subsequently, for each subject, we applied one-way repeated measures analysis of variance to determine if there were significant differences among the segment means; the same procedure was applied to the segment standard deviations. We found no intersegmental differences in either means or standard deviations in the selected data sets, suggesting that all the time series to be analyzed were stationary.

Spectral analysis. A linear interpolation algorithm was first used to convert the RRI into equally spaced measures of heart rate with a new sampling rate of 16 Hz (4). After linear detrending, the power spectrum of HRV was computed from each data segment using the prewhitened autoregressive spectral analysis method of Birch et al. (5). Briefly, this procedure involved the following steps: fitting an autoregressive model to the data; determining the residuals between the measurements and the model predictions; computing the spectrum of the residuals via fast Fourier transform; and, finally, filtering the residuals spectrum with the autoregressive model to obtain the spectrum of variations in RRI. It should be noted that a relatively high resampling rate (16 Hz) was required to obtain good frequency resolution in the resulting spectrum, because this algorithm required the fast Fourier transform of the residuals. Before the spectral computations, a preliminary analysis showed that an autoregressive model of order 10 was adequate for fitting the data.

We obtained compact descriptors of the spectral characteristics of HRV by deducing the power contained in specific frequency bands. These bands were as follows: low-frequency power (LFP), between 0.03 and 0.1 Hz; mid-frequency power (MFP), between 0.1 and 0.2 Hz; and high-frequency power (HFP), between 0.3 and 2 Hz. To gain further insight into the relative contributions of the sympathetic and parasympathetic nervous systems to cardiac autonomic control, we computed the low-to-high frequency ratio (LHR), defined as

$$\mathrm{LHR} = \frac{\mathrm{LFP} + \mathrm{MFP}}{\mathrm{HFP}} \qquad (1)$$

LHR has been used to represent sympathovagal balance, so that an increased value would reflect greater sympathetic modulation and/or reduced vagal modulation of heart rate (31). We also computed the normalized high-frequency power (NHFP), a commonly accepted index of parasympathetic modulation of the heart (31), by dividing HFP by the total spectral power between 0.03 and 2 Hz. Total HRV was assessed by computing the standard deviation (SDRR) of each data set after removal of any linear trend.

Approximate entropy. Approximate entropy (ApEn) is defined as the logarithmic likelihood that the patterns of the data that are close to each other will remain close for the next comparison with a longer pattern. Thus ApEn provides a generalized measure of regularity. A deterministic signal with high regularity has a higher probability of remaining close for longer vectors of the series and hence has a very small ApEn value. On the other hand, a random signal has a very low regularity and produces a high ApEn value.

To compute ApEn of each data set, m-dimensional vector sequences [$\mathbf{x}(n)$] were constructed from the RRI time series

$$\mathbf{x}(n) = [\mathrm{RRI}(n), \ldots \mathrm{RRI}(n + m - 1)] \qquad (2)$$

where the index n can take on values ranging from 1 to $N - m + 1$ and N is the total number of data points in the RRI

time series. If the distance between two vectors $\mathbf{x}(i)$ and $\mathbf{x}(j)$, is defined as $d[\mathbf{x}(i),\mathbf{x}(j)]$, then we have

$$\Phi^m(r) = (N - m + 1)^{-1} \sum_{i=1}^{(N-m+1)} \ln C_i^m(r) \qquad (3a)$$

where $C_i^m(r)$ = {number of $\mathbf{x}(j)$ such that $d[\mathbf{x}(i), \mathbf{x}(j)] \leq r$}/$(N - m + l)$ and r is the tolerance ApEn (m,r,N) is then defined as follows

$$\begin{aligned} \mathrm{ApEn}(m, r, N) &= -[\Phi^{m+1}(r) - \Phi^m(r)] \\ &= -\text{ Average over } i \text{ of ln [conditional probability that} \\ &\quad |\mathrm{RRI}(j + m) - \mathrm{RRI}(i + m)| \leq r, \text{ given that} \\ &\quad |\mathrm{RRI}(j + k) - \mathrm{RRI}(i + k)| \leq r, \text{ for } k = 0, 1, 2, \ldots m - 1] \end{aligned} \qquad (3b)$$

The selection of the parameter m was made such that the conditional probabilities defined in *Eq. 3a* could be estimated with reasonable accuracy from 1,000 data points. On the basis of the work of Pincus et al. (22), this suggested two possibilities: $m = 2$ and $m = 3$. The tolerance r was chosen such that it was larger than most of the noise but, at the same time, not so large that detailed information about the system dynamics would be lost. We found values of r ranging between 10 and 20% of SDRR to be adequate from this perspective.

Correlation dimension. The correlation dimension (CD) describes the dimensionality of the underlying process in relation to its geometrical reconstruction in phase space. We estimated CD using an approach based on the Grassberger-Procaccia algorithm (10). From the RRI time series, the following m-dimensional time-lag vectors were first constructed

$$\mathbf{z}_i = [\mathrm{RRI}(i - \tau), \ldots \mathrm{RRI}(i - m\tau)] \qquad (4)$$

where τ is the embedding lag. For each of the vectors $\mathbf{z}_i$ we computed the distances $\mathbf{z}_i - \mathbf{z}_j$ to all the remaining vector points $\mathbf{z}_j$, excluding those that were close because of temporal correlations (15). The number of data points within a distance r in the phase space for each vector was counted, and this is counted for all $\mathbf{z}_i$. The correlation integral $C(r)$ is given by

$$C(r) = \frac{1}{(N - \eta_{\min})(N - \eta_{\min} - 1)} \sum_{i=1}^{N} \sum_{j=i+\eta_{\min}}^{N} \theta(r - |\mathbf{z}_i - \mathbf{z}_j|) \qquad (5a)$$

where $\eta_{\min}$ is the average correlation time (expressed in units of the number of data points), defined as the time taken for the autocorrelation function to first decay to $1/e$. $\theta(u)$ is the Heaviside function, defined as

$$\begin{aligned} \theta(u) &= 1 \text{ if } u > 0 \\ &= 0 \text{ if } u < 0 \end{aligned} \qquad (5b)$$

$C(r)$ was computed for a range of values of distances r, and, subsequently, log $C(r)$ was plotted against log r. A scaling region was chosen in which this curve was approximately linear, and CD was computed as the slope of the curve in this region

$$\mathrm{CD} = \frac{d[\log C(r)]}{d(\log r)} \qquad (6)$$

The dimension m of the reconstructed vectors was selected by applying the method of false nearest neighbors (26). For the embedding time lag τ, we chose the value of one beat, because this was the natural time scale of the RRI time series (2). We also repeated our analyses with embedding lags of up to six beats (corresponding to the first zero crossing of the autocorrelation functions in most of our data sets), but these did not alter the relative differences of CD among subject groups and sleep states.

Nonlinear predictability. Nonlinear predictability provides a means for detecting determinism in any given time series. Predictability is low for a stochastic time series regardless of how far in the future one tries to predict. On the other hand, a periodic signal is highly predictive. With a chaotic signal or a correlated noise sequence, predictability would be high in the immediate future, but with increasing time steps, predictive capability would decrease significantly.

In this study, we employed a modification of the Sugihara and May method (30). Time-delay vectors were first reconstructed from each RRI signal using the procedures described earlier. The embedded sequence was divided into equal halves, of which the first half was used as the library pattern to make predictions about the behavior of the second half. For a given vector $\mathbf{z}_t$ ("predictee") selected from the second half of the time series, the $m + 1$ vectors located closest (in Euclidean distance) to it were determined from the library patterns so that the predictee was contained in the smallest simplex formed by the $m + 1$ neighbors. The predicted value of the predictee p time steps ahead, x'_{t+p}, was determined by following the time evolution of each of the $m + 1$ closest neighbors. If x_j and $x_j^{(p)}$ $(j = 1 \ldots m + 1)$ represent the first coordinates of each of the $m + 1$ closest neighbors at the current time and after p time steps, respectively, then

$$x'_{t+p} = \sum_{j=1}^{m+1} w_j x_j^{(p)} \qquad (7a)$$

where the weights w_j were chosen to be inversely proportional to the distances between each of the $m + 1$ closest neighbors and the predictee vector $\mathbf{z}_t$, i.e.

$$w_j = \frac{1}{|x_j - x_t|} \left(\sum_{j=1}^{m+1} \frac{1}{|x_j - x_t|} \right)^{-1} \qquad \text{where } \sum_{j=1}^{m+1} w_j = 1 \qquad (7b)$$

As a measure of (non)predictability, we computed the normalized mean square error (ϵ^2). Between the one step ahead ($p = 1$) prediction and its corresponding data value

$$\epsilon^2 = \frac{\Sigma\,(x_{t+1} - x'_{t+1})^2}{\Sigma\,(x_n - \bar{x})^2} \tag{7c}$$

where t is the time index of the predictee, and $\bar{x}$ is the mean value of x.

Detection of nonlinearity using surrogate data. The preceding measures of nonlinear dynamics can be easily corrupted by the presence of stochastic noise. The surrogate data technique provides a means for testing the statistical significance of each computed measure. We employed the amplitude-adjusted Fourier transform algorithm (32) to generate surrogate data sets from the original time series. Here, the original data set was first rescaled so that the distribution became Gaussian. Surrogate data sets of the same length were then generated from this rescaled time series by randomizing the phase components of its Fourier transform while preserving the magnitude of the spectrum. Finally, the Gaussian surrogates were rescaled back to the original amplitude distribution of the data.

For each of the estimated measures of nonlinear dynamics, we computed the significance level (σ) as

$$\sigma = \frac{|Q_r - \mu_{\text{surr}}|}{\sigma_{\text{surr}}} \tag{8}$$

where Q_r is the parameter value for the real data, and μ_{surr} and σ_{surr} are the mean and variance of the surrogates, respectively. A significance level >2 implied that we could reject the null hypothesis that the computed measure reflected linear correlations within the time series being analyzed.

Parametric models. In addition to detecting nonlinearity in the underlying dynamics of HRV, we were also interested in determining the extent of the nonlinearity present. To quantify the degree of nonlinearity, we turned to parametric modeling. Figure 1 shows two possible model structures, both assuming delayed feedback, that can produce the dynamic fluctuations observed in the RRI time series. *Model A* assumes that the feedback dynamics are constrained to be linear, whereas in *model B* the dynamics of the feedback block are nonlinear. In *model A*, aperiodic fluctuations in RRI can only be produced when the feedback system is driven by a stochastic noise input. In contrast, in *model B*, aperiodic fluctuations in RRI can arise with or without any noise perturbation if the system dynamics are chaotic. The feedback structure inherent in both models encapsulates all the deterministic correlation between the present RRI and past changes in RRI. Thus both models represent the totality of all physiological mechanisms that can affect HRV, including respiration. The stochastic noise that enters these systems represents the combined effects of random fluctuations in autonomic neural modulation of heart rate, cardiac contractility, peripheral circulatory resistance, and blood pressure as well as transient variations in sleep-wake state (microarousals).

Model A was represented mathematically by the autoregressive equation

$$\Delta\text{RRI}_n = a_1\Delta\text{RRI}_{n-1} + a_2\Delta\text{RRI}_{n-2} + \cdots a_K\Delta\text{RRI}_{n-K} + e_n \tag{9}$$

where ΔRRI_n represents the change in RRI at beat n from the mean RRI of the data set in question, e_n is the residual error between the nth measurement and the corresponding model prediction, a_i represents the ith model coefficient ($1 \le i \le K$),

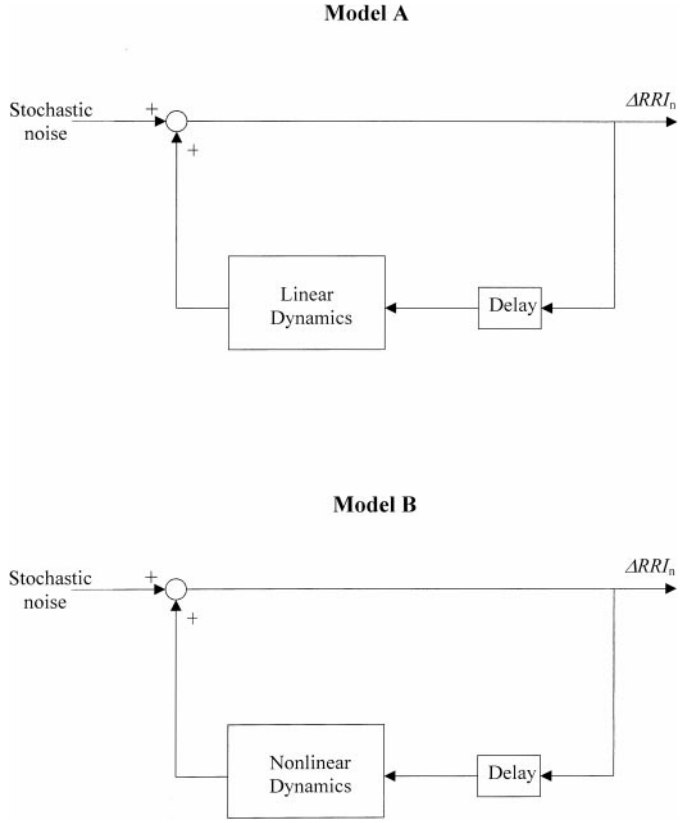

Fig. 1. Parametric models for underlying dynamics of heart rate variability. *Top*: *model A*, linear model; *bottom*: *model B*, nonlinear model. ΔRRI_n, change in R-R interval (RRI) at beat n from the mean RRI of the data set in question.

and K is the model order. In *model B*, we assumed the nonlinear feedback structure to take the form of a d-degree polynomial function

$$\begin{aligned}\Delta\text{RRI}_n = {} & a_1\Delta\text{RRI}_{n-1} + a_2\Delta\text{RRI}_{n-2} + a_K\Delta\text{RRI}_{n-K} \\ & + \cdots a_{K+1}\Delta\text{RRI}^2_{n-1} + a_{K+2}\Delta\text{RRI}_{n-1}\Delta\text{RRI}_{n-2} \\ & + \cdots a_M\Delta\text{RRI}^d_{n-M} + \epsilon_n\end{aligned} \tag{10}$$

M is the total number of unknown parameters to be estimated in *Eq. 10*, where

$$M = \frac{(K+d)!}{d!K!} \tag{11}$$

In *model B*, K was assumed to be equal to the embedding dimension (1), which we computed using the false nearest neighbor algorithm (26). The coefficient a_i ($l \le i \le M$) was estimated from the RRI signal using the Korenberg method (16), which employs a recursive Gram-Schmidt procedure for orthogonal expansion. With the use of simulated data, Korenberg (16) showed that this algorithm produces reliable estimates of the expansion coefficients for data sets of 1,000 points with noise levels as large as 32% of signal amplitude.

In both models, the total number of model parameters to be estimated, M (note that $K = M$ in *model A*), was determined by increasing the number of terms in *Eqs. 9* or *10* until the following information criterion (IC) (1) was minimized

$$IC(M) = \log\left(\frac{1}{N}\sum_{n=1}^{N}\epsilon_n^2\right) + M/N \tag{12}$$

Table 1. *Values for estimated parameters in control and prenatal cocaine-exposed infants in quiet and active sleep*

Estimated Parameter	Cocaine Group		Control Group	
	Quiet sleep	Active sleep	Quiet sleep	Active sleep
Mean RRI, ms	460.90	438.10	435.00	429.9583
SDRR, ms	12.06 ± 1.90	22.60 ± 1.73	9.87 ± 1.26	19.64 ± 2.04
NHFP	0.307 ± 0.061	0.073 ± 0.029	0.314 ± 0.047	0.052 ± 0.005
LHR	1.52 ± 0.60	9.78 ± 1.91	2.23 ± 1.18	9.56 ± 1.21
ApEn	4.90 ± 0.40	2.60 ± 0.32	4.48 ± 0.43	3.49 ± 0.39
CD	4.24 ± 0.66	3.28 ± 0.34	4.21 ± 0.47	3.39 ± 0.54
Prediction error	0.49 ± 0.06	0.32 ± 0.07	0.40 ± 0.14	0.17 ± 0.02

Values are means ± SD. RRI, R-R interval; SDRR, standard deviation of each data set; NHFP, normalized high-frequency power; LHR, low-to-high-frequency ratio; ApEn, approximate entropy; CD, correlation error.

The percent contribution to total variance (CTV) in the data for both models was defined as follows

$$\mathrm{CTV} = \frac{\sum_{n=1}^{N} (\Delta \mathrm{RRI}_n^{\mathrm{predicted}})^2}{\sum_{n=1}^{N} \Delta \mathrm{RRI}_n^2} \times 100 \qquad (13)$$

Once the optimal model order (for *model B*) was determined, the variance of the residuals (ϵ_n) was taken to represent the stochastic contribution to total variance in the data. Thus the variance of ϵ_n provided an estimate of the magnitude of the noise input driving the feedback model (Fig. 1, *bottom*; *model B*).

Statistical analysis. Two-way repeated measures analysis of variance was employed, with subject group (control vs. cocaine) as one factor and sleep state (quiet sleep vs. active sleep) as the repeated factor. A Student-Newman-Keuls test was employed for post hoc multiple pairwise comparisons if statistical significance was indicated by the analysis of variance. All statistical tests were implemented using SigmaStat/Windows (Jandel Scientific; San Rafael, CA). The level of significance was set at $P = 0.05$ unless otherwise stated. In addition, each of the indexes of nonlinear dynamics (i.e., ApEn, CD, and nonlinear predictability) was tested in every subject for significance by computing σ in *Eq. 8* and determining whether the computed value was >2.

RESULTS

Spectral analysis. Table 1 shows the values for the estimated parameters in the two groups of infants in quiet and active sleep. Mean RRI in both groups of infants was not significantly different. There were no group differences in SDRR, LHR, and NHFP. However, NHFP was significantly higher in quiet sleep compared with active sleep in both groups ($P < 0.001$). At the same time, LHR and SDRR were each higher in active sleep relative to quiet sleep ($P < 0.001$ for both).

Approximate entropy. ApEn was not significantly different between the two groups regardless of which combinations of parameters ($m = 2$ or 3 and $r = 10$ or 20%) were employed. However, ApEn was higher in quiet sleep compared with active sleep ($P < 0.001$). The results for the individual subjects for $m = 2$ and $r = 10\%$ are presented graphically in Fig. 2 (cocaine subjects are shown as filled circles, whereas the controls appear as open squares). For each subject, the ApEn value deduced from data (horizontal axis) has been plotted against the mean ($\pm 2\sigma$ confidence intervals, shown as error bars; vertical axis) of the corresponding ApEn values for the 10 sets of surrogates generated from the original time series. Significance levels for the difference in ApEn between the measured RRI and the corresponding surrogate data were >2 in virtually all subjects in both groups and states. In Fig. 2, this result is represented by the fact that almost all the circles and error bars lie above the line of identity, which is the graphical correlate of the null hypothesis. Thus ApEn

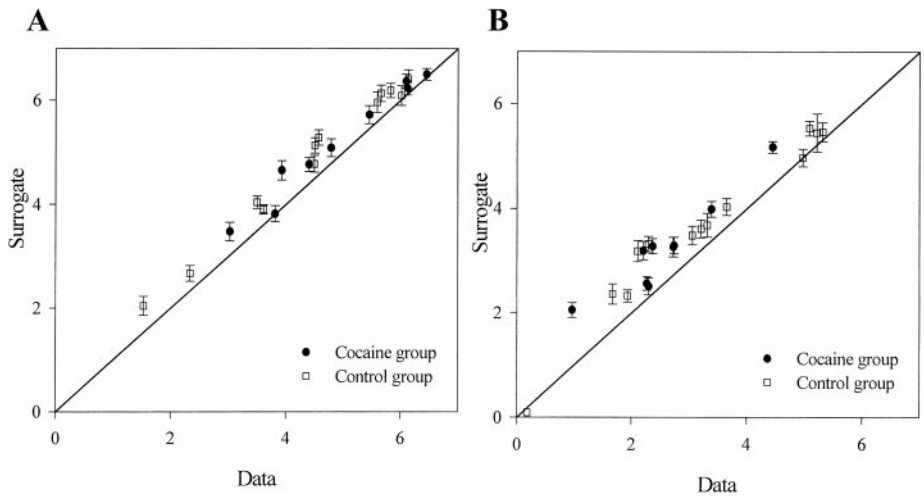

Fig. 2. Results of approximate entropy analysis. *A*: quiet sleep; *B*: active sleep.

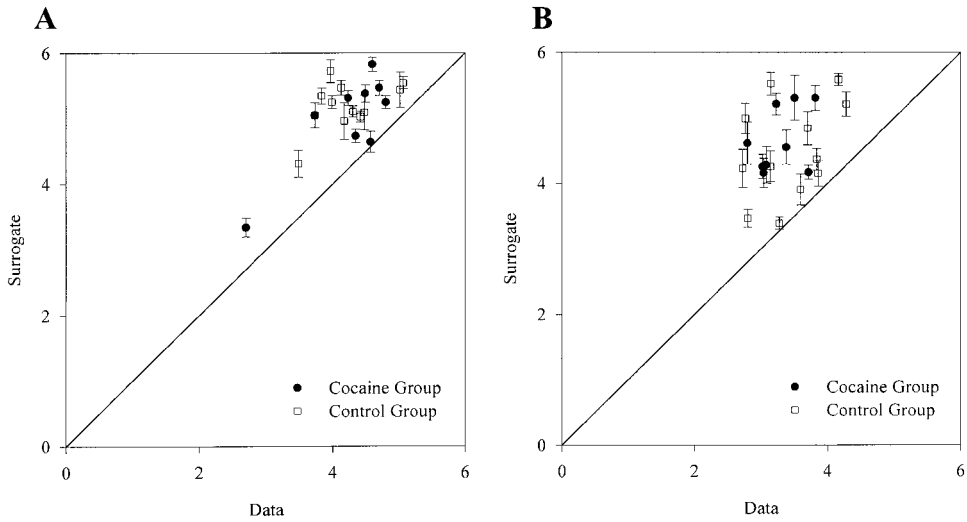

Fig. 3. Results of correlation dimension analysis. *A*: quiet sleep; *B*: active sleep.

values were found to be lower than what would have been expected if the dynamics of the RRI fluctuations reflected only linear correlations. In other words, the time series of all subjects showed a greater degree of regularity as a consequence of nonlinear correlations in the data.

Correlation dimension. The estimated values of CD for the two infant groups in the two sleep states are displayed in Table 1. Group differences were not significant. However, CD was higher in quiet sleep compared with active sleep in both groups ($P < 0.001$). Figure 3 shows the estimated CD values plotted against their corresponding surrogate data values. The surrogate data show higher CD values than the RRI signal itself in both states. The significance factor of this difference in the original data and the surrogate data was $>2\sigma$ for both groups, indicating the contribution of nonlinear correlations in the signal.

Prediction analysis. The normalized variance of the error between the one-step-ahead predictions and their corresponding data values was higher in quiet sleep versus active sleep ($P < 0.001$) but was not significantly different between the cocaine and control subjects (Table 1). Individual prediction errors are plotted against the corresponding prediction errors estimated from the surrogate data sets in Fig. 4. In most of the cases, prediction error is larger in the surrogate data relative to the prediction error deduced from the original data sets, implying again that the nonlinear contribution to the underlying dynamics was significant in both groups of infants in both sleep states.

Parametric model. The number of autoregressive terms that minimized the cost function (*Eq. 12*) for *model A* ranged from 7 to 14. In *model B*, the "optimum" model order contained 36–43 terms, which generally included linear, second-degree, and some third-degree terms. Figure 5 shows the percent CTV for *model A* (*top*) and *model B* (*bottom*) in each individual data set. Statistical analysis showed that there were no differences in CTV between subject groups. However, CTV increased substantially ($P < 0.001$) from *model A* to *model B* in both sleep states. Furthermore, there was a significant state versus model interaction ($P < 0.001$). In quiet sleep, the linear model (*model A*) was able to account for 31.6 ± 5.1% of the dynamic fluctuations in RRI in the cocaine group and 32.6 ± 5.2% in

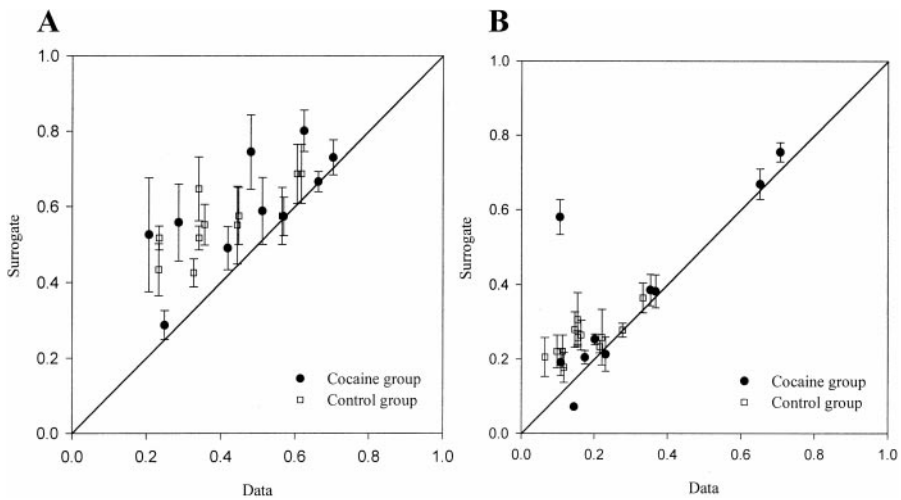

Fig. 4. Results of nonlinear prediction analysis shown as the normalized mean squared error. *A*: quiet sleep; *B*: active sleep.

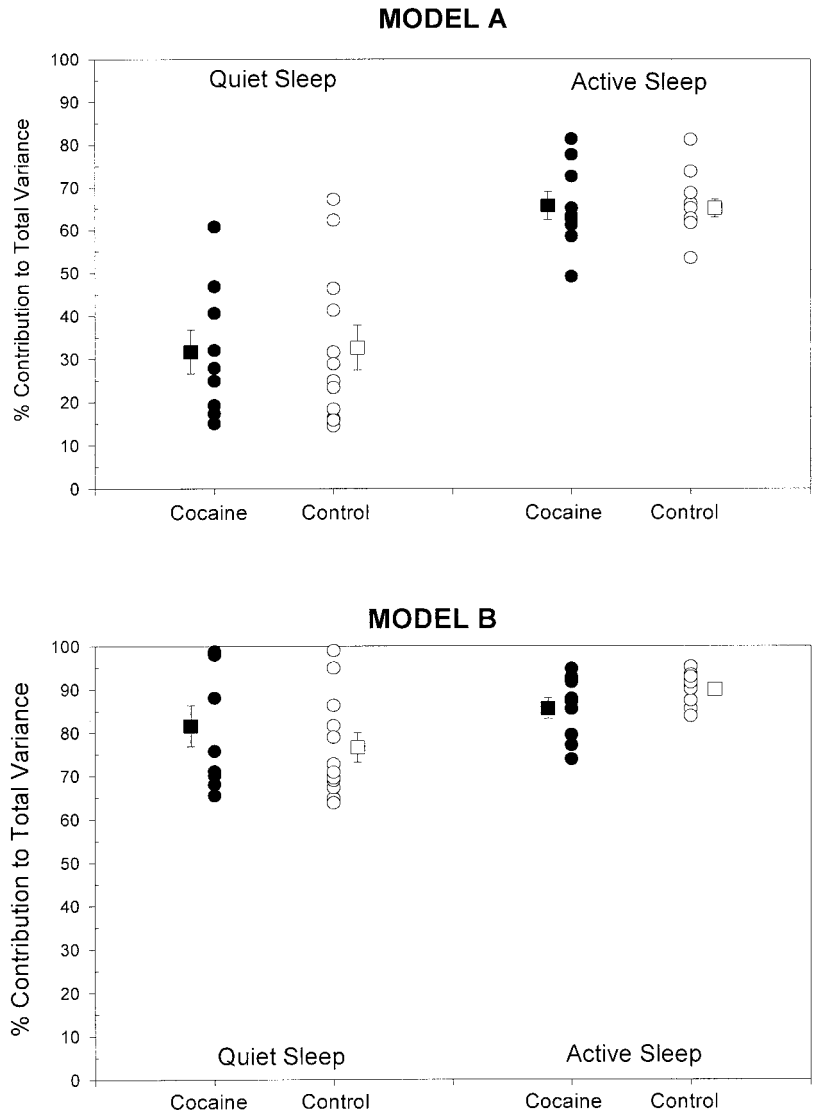

Fig. 5. Results of parametric models shown as percent contribution to total variance. *Top*: *model A*, linear model; *bottom*: *model B*, nonlinear model.

the control group, whereas in active sleep the linear CTV increased to 65.7 ± 3.3 and 65.2 ± 2.1%, respectively. In quiet sleep, CTV for the nonlinear model was 81.5 ± 4.7 and 76.6 ± 3.5% in the cocaine and control groups, respectively. These contributions remained little changed in active sleep at 85.6 ± 2.5 and 89.9 ± 1.0%, respectively. Because *model B* also includes linear terms, these results imply that the nonlinear contribution to RRI dynamics in quiet sleep was substantially larger than that in active sleep. However, there were no differences in nonlinear contributions between infant groups.

DISCUSSION

Two findings emerged with great consistency in this study. First, there was a substantial amount of intersubject variability in all the measures of linear and nonlinear dynamics that were estimated. Second, we could find no significant differences in ApEn, CD, nonlinear predictability, or any of the spectral measures between a group of neonates with prenatal cocaine exposure and a group of age-matched controls. The second finding could well be a consequence of the first: a large degree of intersubject variability can easily mask small differences in heart rate dynamics between the groups. It should be emphasized that the large intersubject variability was found not only in the cocaine-exposed group but also in the control group. Thus it appears that any alterations in heart rate dynamics in cocaine-exposed neonates are likely to be too subtle for detection even by nonlinear techniques unless much larger sample sizes are employed. This could explain why previous studies using spectral analysis of HRV have arrived at differing conclusions. For instance, Mehta et al. (19) reported a significantly lower LHR and higher NHFP in 21 cocaine-exposed neonates, suggesting enhanced parasympathetic activity. Oriol et al. (21) found reduced overall HRV, LFP, and HFP in a group of five cocaine-exposed neonates relative to normal controls, which suggested increased sympathetic tone. On the other hand, they did not find significant differences in ApEn between the groups.

Another confounding factor could be the possible influence of nonstationarity in these previous studies. In the Mehta et al. study (19), the spectral analysis results appear to have been based on data derived from Holter recordings of 22 h or more. Comparison of spectral indexes of HRV between the cocaine infants and controls was performed without consideration of the sleep-wake state. In the Oriol et al. study (21), the data segments analyzed were similar in length (~10 min) to ours. However, only visual inspection was employed to determine stationarity of the data, whereas in our present study we applied statistical testing to rule out any nonstationary behavior.

In our previous analysis of a larger group of 15 cocaine-exposed neonates and 13 controls (inclusive of the subjects studied here), the cocaine infants showed enhanced HRV, reflected by an increase in spectral power across all frequency bands during active sleep; however, in quiet sleep, only HFP was higher (24). The discrepancy between these results and our present findings may be due in part to the slightly larger sample size employed in the previous analysis. In the present study, we were constrained to use only a subset of the overall database because, in some of the subjects, we were not able to find contiguous periods of at least eight (1 min) epochs of quiet or active sleep. The discrepancy may also be related to methodological differences between our previous and present analyses. In the previous study, spectral estimates were computed on an epoch-by-epoch basis. These epochs were classified into one of the following four states: quiet sleep, active sleep, indeterminate sleep, and wakefulness. Subsequently, the median value deduced from all epochs in each state was taken to be representative of the spectral estimate in that state for a given subject. No attention was paid to whether these median values reflected heart rate dynamics during relatively stable and extended periods of a given sleep state. In contrast, in the present study, care was taken to ensure that the data analyzed were extracted from sections in which there were 8–10 contiguous epochs (1 min) of either quiet or active sleep; furthermore, we were careful to test these data segments for stationarity. Because sleep organization is known to be altered in cocaine-exposed infants (25), it is possible that the conclusions arrived at in our previous study may have been affected by the cardiorespiratory effects of transitions between states. If this was indeed the case, our present findings would suggest that the primary effect of prenatal cocaine exposure is the disorganization of sleep architecture and that any observed differences in heart rate control are secondary to these alterations in sleep-state patterning.

Application of the surrogate data method to our estimates of ApEn, CD, and nonlinear predictability showed that there was a significant nonlinear deterministic component in the HRV of both groups of neonates during quiet and active sleep. Parametric modeling confirmed this finding and, furthermore, allowed us to quantify the relative contributions of the linear and nonlinear components of the underlying dynamics. Our results suggest that the dynamic fluctuations in RRI in both cocaine-exposed and control infants can be modeled as the output of a deterministic nonlinear delayed-feedback system with stochastic noise as the perturbing input ("*model B*"). In both infant groups, the nonlinear system was of relatively low order, containing lagged products of ΔRRI up to only the third degree. We found that the combined contributions from linear and nonlinear correlations accounted for between 65 and 99% of the total variance in the data, which meant that in some cases the direct contribution from stochastic noise was as low as 1%. This suggests that, in some of the data sets, the dynamics of HRV may have been chaotic. To test this possibility further, we estimated the largest Lyapunov exponents of these data sets using the method of Rosenstein et al. (27), with the presumption that the presence of a positive characteristic exponent would indicate chaos. We found that these exponents were positive but not significantly different from the Lyapunov exponents computed from the corresponding surrogate data. Thus the determination of whether chaos was present or not was inconclusive. This highlights a major limitation of current methods of nonlinear dynamical analysis: the sensitivity to noise of estimates derived from relatively short (<10,000 points) data sets.

One feature that was continually affirmed in all our computational tests was the clear difference in heart rate dynamics between quiet sleep and active sleep regardless of infant group. Overall HRV was higher in active sleep. NHFP was lower and LHR was higher in active sleep versus quiet sleep, indicating a shift in relative dominance of LFP versus HFP in HRV. All measures of nonlinearity, such as ApEn, CD, and nonlinear prediction error, decreased in active sleep, indicating a reduction in complexity and an increase in regularity in heart rate dynamics. Furthermore, parametric modeling showed that, in percent terms, the linear contribution to HRV was approximately doubled in active sleep, whereas the nonlinear contribution was reduced by roughly one-half. These results are consistent with previous findings that sympathetic modulation of heart rate is enhanced during active or rapid-eye movement sleep, whereas parasympathetic activity is decreased; conversely, in synchronized or quiet sleep, vagal modulation predominates (12, 18). Furthermore, sympathetic modulation leads to dynamic variations of heart rate that are predominantly periodic and in the low-to-mid-frequency range; in contrast, vagal modulation of heart rate produces broadband fluctuations that are dynamically more complex and much less predictable. There are a number of possible reasons why HRV assumes the form of low-frequency periodicities during sympathetic dominance in active sleep. First, the sinoatrial node can only track changes in sympathetic activity that are slower than 0.15 Hz, whereas vagal activity can modulate heart rate to much higher frequencies (28). Sympathetic modulation of changes in vascular resistance is also slow, on the order of several seconds. With increased sympathetic gain, these delays in the baroreflex control

system can lead to oscillatory activity mediated by feedback instability. A less likely, but nevertheless plausible, explanation is that sympathetic dominance during active sleep leads to a filtering out of high-frequency activity, thereby unmasking the low-frequency oscillation that is intrinsic to central rhythmic modulation of neural activity (18).

This work was supported in part by March of Dimes Birth Defects Foundation Grant 12-FY92–0833, by Biomedical Research Support Grant 2S07-RR05780–15, by University of California Los Angeles Academic Senate awards (to M. G. Regalado), and by National Institutes of Health Grants RR-01861 and HL-58725 (to M. C. K. Khoo).

REFERENCES

1. **Barahona M and Poon CS.** Detection of nonlinear dynamics in short, noisy time series. *Nature* 381: 215–217, 1996.
2. **Bassingthwaighte JB, Liebovitch LS, and West BJ.** *Fractal Physiology*. New York: Oxford University Press, 1994, p. 154–158.
3. **Baumgartner W, Hill V, and Bland W.** Hair analysis for drug abuse. *J Forensic Sci* 34: 1433–1453, 1989.
4. **Berger RD, Akselrod S, Gordon D, and Cohen RJ.** An efficient algorithm for spectral analysis of heart rate variability. *IEEE Trans Biomed Eng* 33: 900–904, 1986.
5. **Birch GE, Lawrence PD, Lind JC, and Hare RD.** Application of prewhitening to AR spectral estimation of EEG. *IEEE Trans Biomed Eng* 35: 640–645, 1988.
6. **Chon KH, Kanters JK, Cohen RJ, and Holstein-Rathlou N-H.** Detection of "noisy" chaos in a time series. *Methods Inf Med* 36: 294–297, 1997.
7. **Costa M, Pimentel IP, Santiago T, Sarreira P, Melo J, and Ducla-Soares E.** No evidence of chaos in the heart rate variability of normal and cardiac transplant human subjects. *J Cardiovasc Electrophysiol* 10: 1350–1357, 1999.
8. **Day NL, Wagener DK, and Taylor PM.** Measurement of substance use during pregnancy: methodologic issues. In: *Consequences of Maternal Drug Abuse*, edited by Pinkert TM. Rockville, MD: NIDA Res. Monogr. 59: 36–47, 1985.
9. **Goldberger AL.** Is the normal heartbeat chaotic or homeostatic? *News Physiol Sci* 6: 87–91, 1991.
10. **Grassberger P and Procaccia I.** Characterization of strange attractors. *Physica D* 9: 189–208, 1985.
11. **Guzzetti S, Signorini MG, Cogliati C, Mezzetti S, Porta A, Cerruti S, and Malliani A.** Non-linear dynamics and chaotic indices in heart rate variability of normal subjects and heart-transplanted patients. *C R Seances Soc Biol Fil* 31: 441–446, 1996.
12. **Harper RM, Walter DO, Leake B, Hoffman HJ, Sieck GC, Sterman MB, Hoppenbrouwers T, and Hodgman J.** Development of sinus arrhythmia during sleeping and waking states in normal infants. *Sleep* 1: 33–48, 1978.
13. **Ivanov PC, Amaral LA, Goldberger AL, Havlin S, Rosenblum MG, Struzik ZR, and Stanley HE.** Stochastic feedback and the regulation of biological rhythms. *Europhys Lett* 43: 363–368, 1998.
14. **Kanters JK, Holstein-Rathlou N-H, and Agner E.** Lack of evidence for low-dimensional chaos in heart rate variability. *J Cardiovasc Electrophysiol* 5: 591–601, 1994.
15. **Kantz H and Schreiber T.** *Nonlinear Time Series Analysis*. Cambridge, UK: Cambridge University Press, 1997, p. 72–75.
16. **Korenberg M.** Identifying nonlinear difference equation and functional expansion representations: the fast orthogonal algorithm. *Ann Biomed Eng* 16: 123–142, 1988.
17. **Littman B and Parmalee AH.** Medical correlates of infant development. *Pediatrics* 61: 470–74, 1978.
18. **Mancia G.** Autonomic modulation of the cardiovascular system during sleep. *N Engl J Med* 328: 347–349, 1993.
19. **Mehta SK, Finkelhor RS, Anderson RL, Harcar-Sevcik RA, Wasser TE, and Bahler RC.** Transient myocardial ischemia in infants prenatally exposed to cocaine. *J Pediatr* 122: 945–949, 1993.
20. **Needleman R, Frank DA, Augustyn M, and Zuckerman BS.** Neurophysiological effects of prenatal cocaine exposure: comparison of human and animal investigations. In: *Mothers, Babies, and Cocaine: the Role of Toxins in Development*, edited by Lewis M and Bendersky M. Hillsdale, NJ: Lawrence Erlbaum, 1995, p. 229–250.
21. **Oriol N, Bennett F, Rigney D, and Goldberger A.** Cocaine effects on neonatal heart rate dynamics: preliminary findings and methodological problems. *Yale J Biol Med* 66: 75–84, 1993.
22. **Pincus SM, Cummins TR, and Haddad G.** Heart rate control in normal and aborted-SIDS infants. *Am J Physiol Regulatory Integrative Comp Physiol* 264: R638–R646, 1993.
23. **Regalado M, Schechtman V, Del Angel P, and Bean X.** Cardiac and respiratory patterns during sleep in cocaine-exposed neonates. *Early Hum Dev* 44: 187–200, 1996.
24. **Regalado M, Schechtman V, Khoo MCK, Shin J, and Bean X.** Sources of heart rate variation during sleep in cocaine exposed neonates. *Ann NY Acad Sci* 846: 415–418, 1998.
25. **Regalado MG, Schechtman VL, Del Angel AP, and Bean X.** Sleep disorganization in cocaine-exposed neonates. *Infant Behav Dev* 18: 319–327, 1995.
26. **Rhodes C and Morari M.** False nearest neighbors algorithm and noise-corrupted time series. *Physiol Rev* 55: 6162–6170, 1997.
27. **Rosenstein MT, Collins JJ, and De Luca CJ.** A practical method for calculating largest Lyapunov exponents from small data sets. *Physica D* 65: 117–134, 1991.
28. **Saul JP, Berger RD, Albrecht P, Stein SP, Chen MH, and Cohen RJ.** Transfer function analysis of the circulation: unique insights into cardiovascular regulation. *Am J Physiol Heart Circ Physiol* 261: H1231–H1245, 1991.
29. **Sugihara G, Allan W, Sobel D, and Allan KD.** Nonlinear control of heart-rate variability in human infants. *Proc Natl Acad Sci USA* 93: 2608–2613, 1996.
30. **Sugihara G and May RM.** Nonlinear forecasting as a way of distinguishing chaos from measurement error in time series. *Nature* 344: 734–741, 1990.
31. **Task Force of the European Society of Cardiology and the North American Society of Pacing and Electrophysiology.** Heart rate variability: standards of measurement, physiological interpretation, and clinical use. *Circulation* 93: 1043–1065, 1996.
32. **Theiler J, Eubank S, Lontin A, Galdrikian B, and Farmer JD.** Testing for nonlinearity in time series: the method of surrogate data. *Physica D* 58: 77–94, 1992.
33. **Woo M, Chang M, Bautista D, Keens T, and Davidson-Ward S.** Elevated heart rates in infants of cocaine abusing mothers during normoxia and hypoxia (Abstract). *Am Rev Respir Dis* 141: 908A, 1990.